Second Prize

Elastographic Measurements of *in-Vivo* Radiofrequency Ablation Lesions of the Kidney

GYAN PAREEK, M.D.,[1] ERIC R. WILKINSON, M.D.,[1] SHYAM BHARAT, B.E.,[2] TOMY VARGHESE, Ph.D.,[2]
PAUL F. LAESEKE, M.D.,[3] FRED T. LEE JR., M.D.,[4] THOMAS F. WARNER, M.D.,[3]
JAMES A. ZAGZEBSKI, Ph.D.,[2] and STEPHEN Y. NAKADA, M.D.[1]

ABSTRACT

Background and Purpose: Elastography may prove useful for monitoring radiofrequency ablative (RFA) therapy because heat-ablated tissues are more elastic than untreated tissues. Herein, we report our initial evaluations of the reliability of elastography for delineating thermal-lesion boundaries at the time of RFA of porcine kidneys.

Materials and Methods: *In-vivo* RFA was performed on 20 kidneys from 10 40-kg female pigs. Elastography was performed at the time of surgery and after 48 hours. The imaging plane was perpendicular to the axis of the RF electrode so that the ablated region was around the center of the plane. Measurements of the sections representing the same image plane used for elastography were taken at pathologic examination and compared with the measurements obtained from the elastograms.

Results: We found a statistically significant correlation between elastography and pathology measurements with respect to the area and volume estimates (r = 0.9302 and r = 0.953, respectively). Overall, elastography slightly underestimated the lesion size, as judged by the digitalized pathologic images, a finding consistent with previous reports.

Conclusion: We found a correlation between the area and volume estimates of thermal lesions that were based on elastographic images and the measurements from gross pathologic dimensions. A a significant limitation of renal RFA is the inaccuracy of current imaging modalities to provide real-time monitoring, and elastography may prove to be reliable for delineating the resulting thermal lesions.

INTRODUCTION

APPROXIMATELY 35,000 CASES of renal-cell carcinoma (RCC) were diagnosed in 2004, representing a 30% increase in the incidence of RCC over the last decade.[1] The increased incidence, characterized by smaller, localized lesions on initial presentation, has been attributed to the widespread use of ultrasongraphy and CT. The stage migration to smaller tumors has also led to a paradigm shift in the management of RCC, evidenced by the increase in the number of patients offered nephron-sparing surgery for cancer control.[2]

Recently, radiofrequency ablation (RFA) has been used by many centers to treat selected patients with small renal masses.[3,4] This technique is favored because it is minimally invasive while being hemostatic and of relatively low cost.[3,4] The RF energy heats tissue by applying alternating current, resulting in ionic agitation. Clinical studies are ongoing, but early evidence suggests that RFA is generally safe, and the oncologic results are encouraging.[3–10] A significant limitation of RFA remains the difficulty of real-time monitoring during therapy. Both CT and MRI have been used to guide treatment, with MRI providing the best tissue-to-tumor contrast and the ability to use

Departments of [1]Surgery/Division of Urology, [2]Medical Physics, [3]Pathology, and [4]Radiology, University of Wisconsin Medical School, Madison, Wisconsin.

multiplanar guidance.[8] However, MRI guidance for ablation is expensive, requires dedicated interventional MRI equipment, and is the least available technology for real-time monitoring. Currently, ultrasonography is the most widely used modality world-wide to monitor RFA, but it is unable to delineate lesion margins because of the production of water vapor during treatment. Thus, real-time monitoring during RFA is difficult, leading to uncertainty about the precise zone of ablation at the time of treatment. Also, complications such as adjacent-organ injury from treating peripheral lesions and collecting-system injury from treating central lesions have been reported.[11]

Recently, there has been enthusiasm about imaging tissue elasticity.[12,13] One of these techniques, elastography, has been useful in monitoring the impact of ablative therapy. Elasticity changes have been demonstrated after RFA and are attributed to protein denaturation from the elevated temperatures during treatment.[10] In the liver, RF lesions exhibit extremely high contrast on elastographic ultrasound images compared with normal, untreated, liver tissue.[14] The experiences from these studies and preliminary data from our institution suggest that sonographic elastography may be substantially superior to conventional sonography for monitoring RFA lesions.

The purpose of our study was to investigate the feasibility of elastography during ablative therapy, performed by monitoring phase changes in the echo signals caused by speed of sound variations and thermal expansion with temperature. We hypothesized that sonographic elastography may provide real-time monitoring and significantly improve the efficacy of RFA in treating renal lesions.

MATERIALS AND METHODS

Animals, anesthesia, and procedures

Twenty female domestic pigs (mean weight 40 kg) were used after approval was obtained from the Research Animal Care and Use Committee of our institution. All husbandry and experimental studies were compliant with the National Institutes of Health *Guide for Care and Use of Laboratory Animals* (http://oacu.od.nih.gov/regs/guide/guidex.htm). Anesthesia was induced with intramuscular tiletamine hydrochloride and zolazepam hydrochloride (Telazol; Fort Dodge, IA), atropine (Phoenix Pharmaceutical, St. Joseph, MO), and xylazine hydrochloride (Xyla-Ject; Phoenix Pharmaceutical). Animals were intubated, and anesthesia was maintained with inhaled isoflurane (Halocarbon Laboratories, River Edge, NJ) to effect. The pigs were placed in the supine position and prepared in the midline and draped. Serum creatinine measurements were obtained prior to beginning the procedure. Through a midline incision, one kidney was dissected free and the lower pole exposed. Following the protocol described below, the identical procedure was performed on the contralateral side.

RFA technique

All 20 RF procedures were performed with the Cool-tip™ system (Valleylab, Boulder, CO). The system includes a 480-kHz monopolar RF generator that operates at a maximum of 200 W (2.0 A at 50 Ω). The generator uses an impedance feedback loop to maximize energy delivery by minimizing charring.

Tissue charring is limited by circulation of chilled sterile water (approximately 18–20°C at the electrode tips) through the electrodes during the ablations by way of a peristaltic pump. The single RF electrodes are 17 gauge (1.5 mm) in diameter with a 3.0-cm exposed tip. Single ablation zones were created by applying power for 12 minutes per ablation according to the manufacturer's recommendations.

Ultrasound monitoring

The ultrasound machine utilized to guide the RF probe placement was an Ultrasonix 500RP real-time scanner (Ultrasonix Medical Corporation, Bothell, WA, and Vancouver, BC, Canada) equipped with a 5-MHz center frequency linear-array transducer with an approximately 60% bandwidth. After treatment, the kidney was allowed to cool to body temperature, the visible lesion was measured, and the kidney was replaced *in situ*.

The pigs were allowed to survive for 48 hours to better evaluate cell death and then sacrificed. Forty-eight hours allows coagulative necrosis to be identified by light microscopy.[15,16] The kidneys were harvested and fixed in 10% Formalin solution after computation of elastographic measurements.

Elastographic measurements

Elastographic imaging was performed using a set-up including a stepper motor, ultrasound probe, and a kidney encased in a gelatin phantom, which was used to provide a regular surface for external quasistatic compression (Figs. 1 and 2). As previously described, the phantoms were prepared using 200-bloom calfskin.[14] Data acquisition to obtain the precompression and postcompression RF signals for elastography was performed using an SSD 2000 real-time scanner (Aloka, Tokyo, Japan) with a 40-mm 7.5-MHz linear-array transducer with a 70% bandwidth. The ultrasound RF signals were then digitized utilizing a 12-bit data-acquisition board (Gage Applied Inc., Montréal, Québec, Canada) at a sampling rate of 100 MHz. The apparatus includes a stepper-motor-controlled motion-compression system and a compression plate that also supports the transducer. Both the transducer and the compression plate are placed in direct contact with the gelatin block. After compression of the gelatin block containing the excised kidney to ensure proper contact, the RF frame is acquired, and the stepper motor is activated to compress the sample, with the postcompression frame acquired immediately and in synchrony with the compression. A personal computer was used to control the operation of the system.

Local tissue-displacement information was estimated from the gated precompression and postcompression RF signals from the location of the normalized cross-correlation function peak. Subsample peak locations were calculated using parabolic interpolation. A window length of 3 mm with a 75% overlap was used to obtain the tissue displacements. Strain estimates were obtained using a five-point linear least-squares fit on the estimates of tissue displacement. A 5×5 median filter was used to reduce strain outliers in the strain image or elastogram.

The ablation zone size was analyzed using the freeware ImageJ (National Institute of Mental Health, Bethesda MD). The lesion areas and volumes were estimated by drawing contours of the lesion shape and then computing the area and volume of
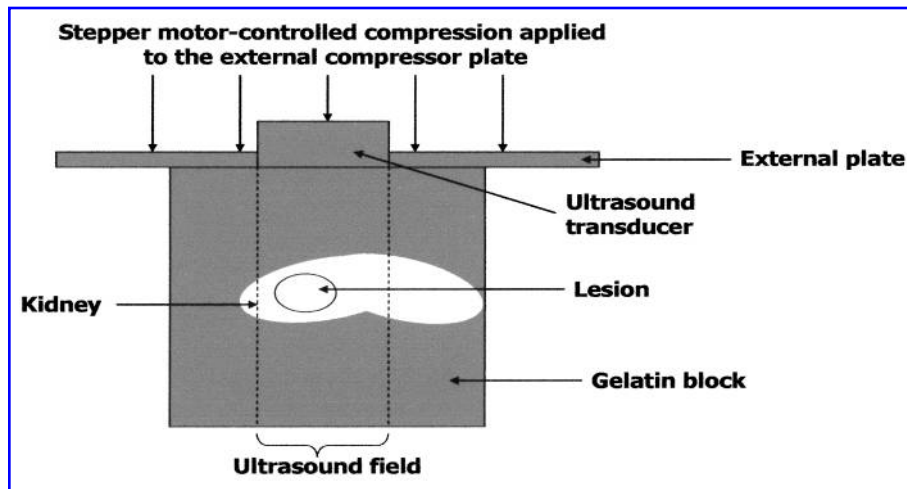
FIG. 1.   System utilized to formulate elastograms.

the bounding ellipse using the formula for the area of an ellipsoid, π ab/4, where a and b are the length and width axis radius. Ablation-zone volumes were calculated using the formula for the volume of an ellipsoid, $4/3\pi$ abc, where a, b, and c are the length, width, and height axis radii, respectively. Maximum ablation zone length, height, and depth were used for these values.

Pathology measurements

The kidneys were cut into 2.4-mm slices on a commercial meat slicer. Slices were optically scanned (Perfection 2450 Photo Model G860A; Epson, Long Beach, CA) and saved as electronic images. The ablation-zone size was analyzed using ImageJ. Ablation-zone measurements were taken using the central, white zone of complete necrosis, not the surrounding red zone that has been shown to contain viable cells. Ablation-zone areas were calculated using the formula for the area of an ellipsoid, and ablation-zone volumes were calculated using the formula for the volume of an ellipsoid. Grossly, the estimated depth of the lesion was calculated by multiplying the number of slices demonstrating a lesion by 0.24 (the thickness of each slice) and summing these values for each kidney.

Histologic analysis

Samples of lesions were embedded in paraffin, stained with hematoxylin and eosin (H&E), and reviewed by a pathologist blinded to the treatment (TFW) for determination of cell death, inflammatory changes, and vascular thrombosis. Examination of the specimen for viable cells and skip lesions was included in the analysis.

Statistical methods

To determine whether the pathology and elastography examinations were giving us the same estimates of lesion area and lesion volume, we tested for differences between the estimates using a Wilcoxon signed-ranks test and determined the strength of the correlation between the estimates using a Spearman correlation coefficient. All analyses were performed using SAS statistical software (SAS Institute Inc., Cary, NC).

RESULTS

A representative elastogram, sonographic B-mode image, and digitalized pathology photograph of a typical RF lesion are illustrated in Figure 3. A three-dimensional (3D) depiction of a thermal lesion was generated from parallel multislice elas-
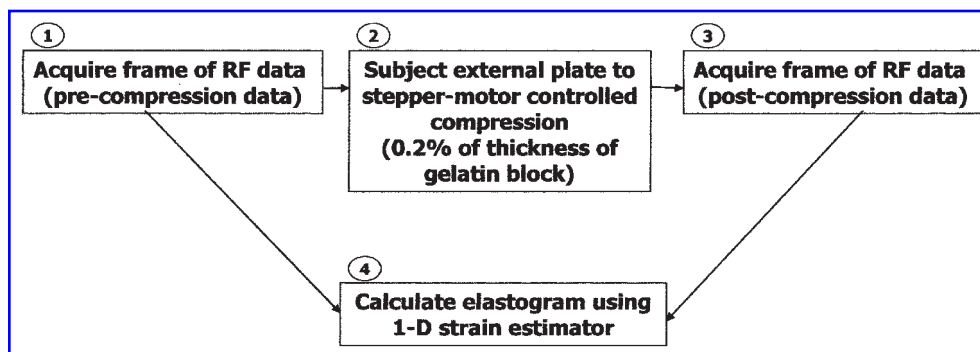

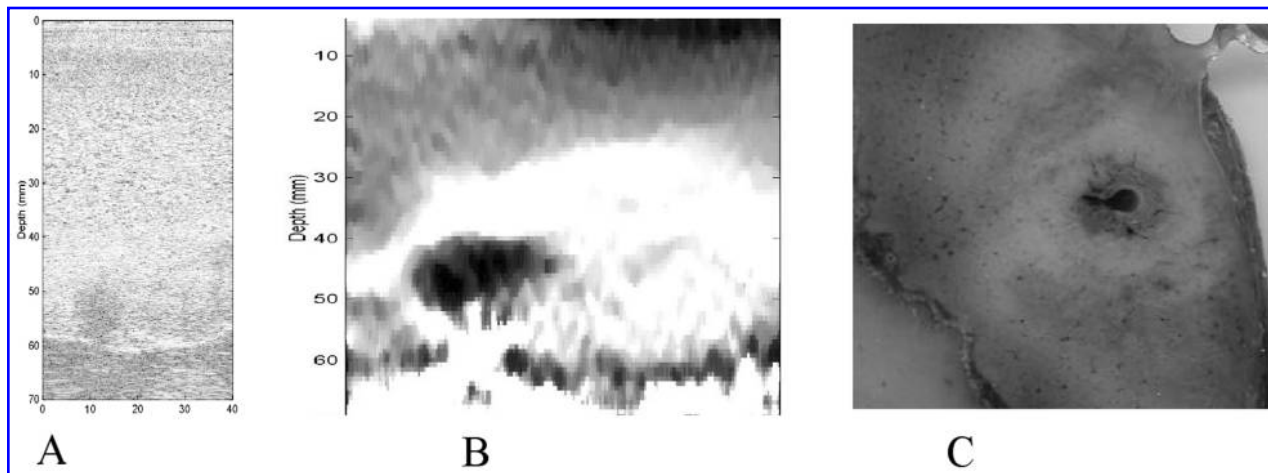**FIG. 2.**   Methodology utilized in formulating elastograms.

FIG. 3. Images of RFA lesion in section of kidney tissue, as seen by (**A**) B-mode ultrasonography, (**B**) elastogram, and (**C**) digitalized photograph of pathologic lesion.

tograms acquired at 1-mm increments (Fig. 4). The 3D representation allows computation of lesion volume.

Thermal-lesion areas and volumes for the 20 ablations were compared to analyze correspondence between elastographic and digitized photographic depictions. All comparisons were made at the corresponding elastographic and pathologic planes for a single representative slice.

Area and volume measurements

A strong correlation of the estimates of areas obtained from elastography and those obtained from gross pathology specimens was observed (r = 0.9302) (Fig. 5A). The correlation ob-

served between the elastographic and pathologic volume estimates was 0.953 (Fig. 5B).

Radiofrequency data

An average temperature of 79°C was obtained at the end of the 20-minute ablation procedures. There was no significant difference between the pretreatment and post-treatment creatinine concentrations ($P = 0.33$).

Histologic analysis

The necrotic zones of the 20 lesions were surrounded by a mean of 1 mm of congestion and intertubular hemorrhage.
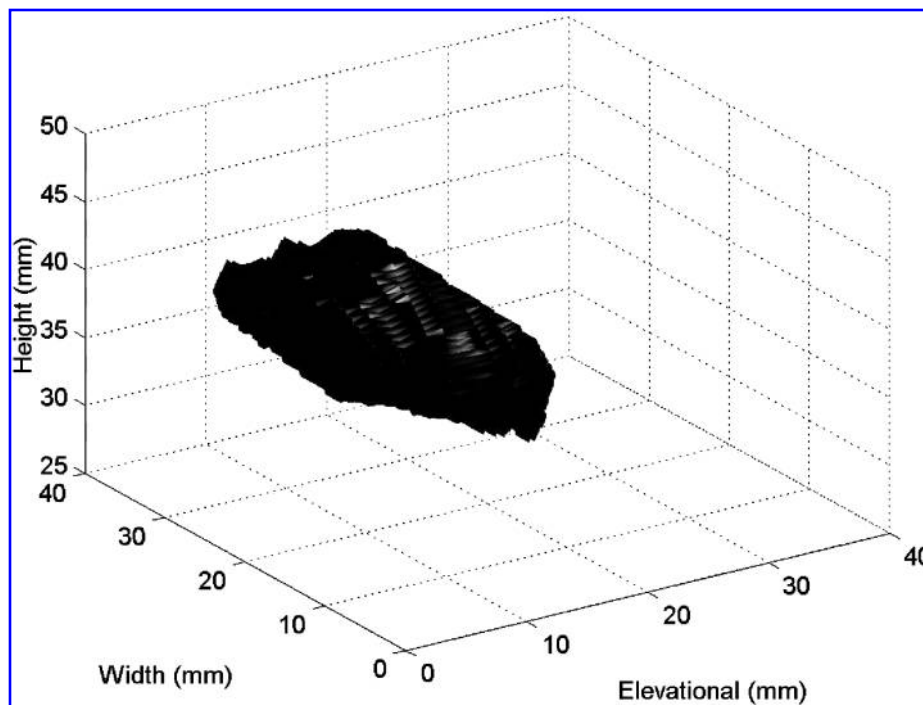

FIG. 4. Three-dimensional elastogram of RFA thermal lesion in porcine kidney.
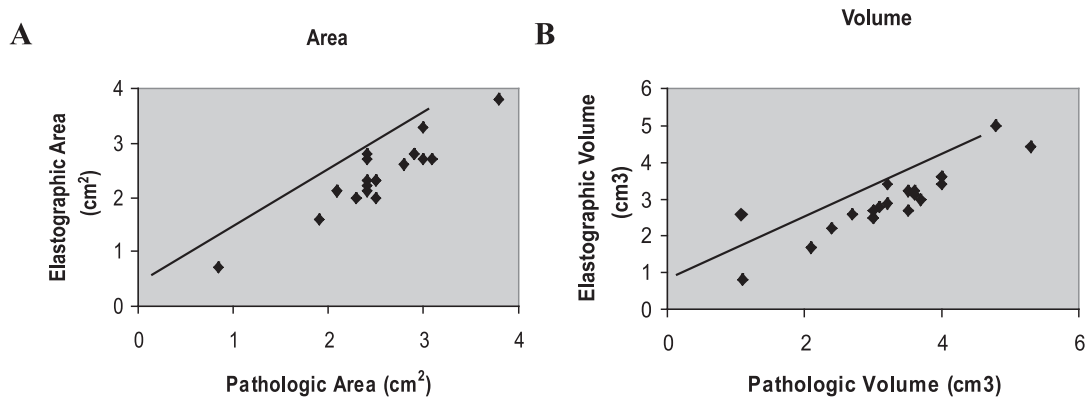
FIG. 5. Scatterplots of (**A**) lesion areas and (**B**) lesion volumes between pathology and elastography and their linear fits.

Tubular and glomerular outlines were intact in the necrotic zone with the exception that cell borders were ablated, and this zone was devoid of erythrocytes. Closer to the zone of hemorrhage, necrosis was more extensive, and tubular outlines and nuclei were faint. These advanced changes were present on either side of an infiltrate of polymorphonuclear leukocytes, which included a zone of hemorrhage. Focal calcification of necrotic cells was present in tubules at the interface with intact uninvolved renal parenchyma. Generally, the tissue around the probe consisted of concentric laminated and elongated tubules. Irregular spaces in this area represented gas bubbles (Fig. 6).

DISCUSSION

Radiofrequency ablation is currently presented as an optional treatment to some patients with renal pathology. The procedure creates thermal lesions by achieving temperatures >60°C, resulting in uniform tissue necrosis.[15,16] A serious limitation of this procedure is the inability to delineate the boundary of an ablated lesion in real time. Radiologic–pathologic correlations in both experimental and clinical studies have demonstrated that CT and
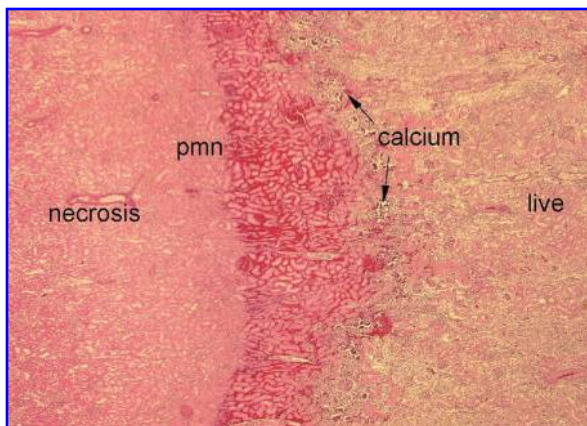

FIG. 6. Ablated kidney excised at 48 hours showing necrotic zone, zone of polymorphonucleocyte (pmn) infiltration, and area of calcium deposition abutting intact kidney tissue. (Hematoxylin & eosin; original magnification ×20).

MRI may aid clinicians in predicting the region of coagulation within 2 to 3 mm following RFA.[17,18] Cha and associates[19] compared the usefulness of CT and sonography as modalities for monitoring RFA and concluded that on CT, RF lesions consistently showed lower attenuation than surrounding tissue. On sonography, the echogenicity of lesions varied, with approximately 59% of the lesions being hypoechoic, 25% hyperechoic, and 16% isoechoic. Thus, a major limitation of this technique is the inability to see the zone of necrosis during treatment because of the intrinsically low contrast between treated and untreated tissue. Further compounding the problem are imaging artifacts seen on ultrasonography as a result of water-vapor formation during the ablation.

Techniques for real-time imaging during RFA have become an important area of research. Recently, a major focus by investigators has been on imaging the change in the elastic properties of tissue that result at the time of RFA.[12–14] Thermal injury resulting from RFA increases the strain or stiffness of tissue because of the elevated temperatures and protein denaturation. These local strain changes may be measured by ultrasonography and displayed as images called "elastograms." Although elastograms generally are obtained using off-line processing, researchers have demonstrated real-time applications using faster algorithms. Recently, Varghese and colleagues[14] demonstrated the feasibility of elastography in monitoring RFA of porcine liver. Those investigators found an excellent correlation between the measurements of the dimensions, areas, and volumes of thermal lesions that were based on elastographic images and measurements based on digital pathologic images. When comparing the digitized pathologic measurements, elastographic measurements showed a tendency to slightly underestimate both the areas and the volumes of lesions. Those investigators concluded that elastography was a reliable technique for delineating thermal lesions resulting from RFA.

We studied the feasibility of elastography as an imaging technique to monitor RFA of renal lesions. We generated elastograms at 48 hours after RFA and compared them with the gross pathologic lesions resulting from the treatment. The survival time allowed coagulative necrosis to become apparent at the light-microscopic level, permitting more accurate depiction of the lesion created by the ablation. Our hypothesis was that tissue that had been ablated could be discriminated from normal tissue by elastography, providing the potential for real-time monitoring during RFA of renal lesions

The elastograms generated in our study displayed with extremely high contrast on ultrasonography compared with normal kidney, allowing clear delineation of the treatment zone. Similar findings have been observed in liver studies.[14] Additionally, we found elastographic measurements of the RF-ablated regions of the kidney correlated well with measurements of the gross pathologic lesions. In our statistical results, the correlation coefficient between the elastographic and pathologic lesion areas was approximately 0.93. The comparison with elastographic and pathologic volumes provided an even stronger correlation: a correlation coefficient of 0.95. Generally, elastography slightly underestimated the lesion size observed on gross pathology, a finding previously reported in liver studies.[14] A possible explanation for the elastographic underestimation could be an accurate reflection of the stiffness of the resulting lesion. Specifically, because elastograms reflect a map of the tissue strain after RFA, the lesion edges may not be as stiff as the core of the lesion. Thus, these strain differences, from the core to the edge of the lesion, may represent a true reflection of the stiffness changes that occur from RFA. Further investigations are needed to substantiate these conclusions.

The accuracy of elastographic measurements demonstrated in our study may alleviate some of the limitations of current modalities utilized to guide RFA, including steam-bubble formation on standard B-mode sonography, as well as the post-treatment artifact seen on standard CT. We postulate that real-time elastography during RFA may increase treatment efficacy, possibly permitting eradication of viable tissue in the treatment zone and preventing the undertreatment of the targeted lesion.

We concede that a limitation of the study is the use of elastographic measurements calculated from directly placing the ultrasound transducer on the kidney, rather than from a percutaneous approach. We believe these measurements were appropriate for initial analysis in our feasibility study, and future *in-vivo* investigations will be performed percutaneously.

Our study demonstrates that elastography is a reliable noninvasive technique that may allow clinicians to assess treatment efficacy at the time of the procedure rather than from the traditional post-treatment imaging. We believe that the strong correlation between elastographic and pathologic thermal lesions in this study warrants further investigation of the *in-vivo* utility of elastography during RFA. Investigations are continuing, and preliminary results are encouraging for real-time monitoring during RFA.

CONCLUSION

Our feasibility study suggests that elastography may be a reliable technique for monitoring the zone of RFA of renal lesions. Our data indicate a significant correlation between elastographic and gross pathologic measurements 48 hours after ablation. We believe our findings demonstrate a significant advancement in the movement toward improving the efficacy of RFA. *In-vivo* studies will be needed to provide data on the utility of elastography for providing real-time monitoring during RFA.

REFERENCES

1. Jemal A, Tiwari RC, Murray T, et al. Cancer statistics 2004. CA Cancer J Clin 2004;54:8–29.
2. Licht MR, Novick AC. Nephron sparing surgery for renal carcinoma. J Urol 1993;149:1–7.
3. Zlotta AR, Wildschutz T, Raviv G, et al. Radiofrequency interstitial tumor ablation (RITA) is a possible new modality for treatment of renal cancer: *Ex-vivo* and *in-vivo* experience. J Endourol 1997;11:251–258.
4. Pavlovich CP, Walther MM, Choyke PL, et al. Percutaneous radio frequency ablation of small renal tumors: Initial results. J Urol 2002;167:10–15.
5. Gervais DA, McGovern FJ, Wood BJ, et al. Radio-frequency ablation of renal cell carcinoma: Early clinical experience. Radiology 2000:665–672.
6. Rendon RA, Kachura JR, Sweet JM, et al. The uncertainty of radio frequency treatment of renal cell carcinoma: Findings at immediate and delayed nephrectomy. J Urol 2002;167:1587–1592.
7. De Baere T, Kuoch V, Smayra T, et al. Radio frequency ablation of renal cell carcinoma: Preliminary clinical experience. J Urol 2002;167:1961–1964.
8. Solbiati L, Ierace T, Goldberger SN, et al. Percutaneous US-guided radio-frequency tissue ablation of liver metastases: Treatment and follow-up in 16 patients. Radiology 1997;202:195–200.
9. Goldberg SN, Gazelle GS, Mueller PR. Thermal ablation therapy for focal malignancy: A unified approach to underlying principles, techniques, and diagnostic imaging guidance. AJR Am J Roentgenol 2000;174:323–331.
10. Hall WH, McGahan JP, Link DP, et al. Combined embolization and percutaneous radiofrequency ablation of a solid renal tumor. AJR Am J Roentgenol 2000;174:1592–1594.
11. Weizer AZ, Raj VG, O'Connell M, et al. Characteristics of patients with complications following percutaneous radiofrequency ablation of renal tumors [abstract]. J Urol 2005;173(suppl):26.
12. Varghese T, Zagzebski JA, Chen Q, et al. Ultrasound monitoring of temperature change during radio-frequency ablation: Preliminary in-vivo results, Ultrasound Med Biol 2002;28:321–329.
13. Varghese T, Zagzebski JA, Frank G, et al. Elastographic imaging using a handheld compressor. Ultrasonic Imaging 2002;24:25–35.
14. Varghese T, Techavipoo U, Liu W, et al. Elastographic measurements of the area and volume of thermal lesions resulting from radiofrequency ablation. AJR Am J Roentgenol 2003;181:701–707.
15. Rosner GL, Clegg ST, Prescott DM, et al. Estimation of cell survival in tumors heated to non-uniform temperature distributions. In J Hyperthermia 1996;12:223–239.
16. Zervas NT, Kuwayama A. Pathologic characteristics of experimental thermal lesions: Comparison of induction heating and radiofrequency electrocoagulation. J Neurosurg 1972;37:418–422.
17. Aschoff AJ, Sulman A, Martinez M, Duerk JL, Resnick MI, MacLennan GT, Lewin JS. Perfusion-modulated MR imaging guided radiofrequency ablation of the kidney in a porcine model. AJR Am J Roentgenol 2001;177:151–158.
18. Goldberg SN, Gazelle GS, Solbiati L, et al. Ablation of liver tumors using percutaneous RF therapy. AJR Am J Roentgenol 1998;170:1023–1028.
19. Cha CH, Lee FT Jr, Gurnry JM, et al. CT versus sonography for monitoring RFA in a porcine liver. AJR Am J Roentgenol 2000;175:705.

Address reprint requests to:
Stephen Y. Nakada, M.D.
Dept. of Surgery, Div. of Urology
University of Wisconsin Medical School
G5/339 Clinical Science Center
600 Highland Avenue
Madison, WI 53792-3236

E-mail: nakada@surgery.wisc.edu

ABBREVIATIONS USED

CT = computed tomography; MRI = magnetic resonance imaging; RFA = radiofrequency ablation.

This article has been cited by:

1. Efstathios T. Detorakis, Eleni E. Drakonaki, Miltiadis K. Tsilimbaris, Ioannis G. Pallikaris, Spiridon Giarmenitis. 2010. Real-Time Ultrasound Elastographic Imaging of Ocular and Periocular Tissues: A Feasibility Study. *Ophthalmic Surgery, Lasers, and Imaging* **41**:1, 135-141. [CrossRef]

2. Hao Chen, Tomy Varghese. 2009. Multilevel hybrid 2D strain imaging algorithm for ultrasound sector/phased arrays. *Medical Physics* **36**:6, 2098. [CrossRef]

3. Rodrigo G Nascimento, Jonathan Coleman, Stephen B Solomon. 2008. Current and future imaging for urologic interventions. *Current Opinion in Urology* **18**:1, 116-121. [CrossRef]

4. Man Zhang, Benjamin Castaneda, Jared Christensen, Wael Saad, Kevin Bylund, Kenneth Hoyt, John G. Strang, Deborah J. Rubens, Kevin J. Parker. 2008. Real-time sonoelastography of hepatic thermal lesions in a swine model. *Medical Physics* **35**:9, 4132. [CrossRef]